An Objective, Information-Based Approach for Selecting the Number of Muscle Synergies to be Extracted via Non-Negative Matrix Factorization

S. Ranaldi, C. De Marchis, G. Severini, S. Conforto

***Abstract*—Muscle synergy analysis is a useful tool for the evaluation of the motor control strategies and for the quantification of motor performance. Among the parameters that can be extracted, most of the information is included in the rank of the modular control model (i.e. the number of muscle synergies that can be used to describe the overall muscle coordination). Even though different criteria have been proposed in literature, an objective criterion for the model order selection is needed to improve reliability and repeatability of MSA results. In this paper, we propose an Akaike Information Criterion (AIC)-based method for model order selection when extracting muscle synergies via the original Gaussian Non-Negative Matrix Factorization algorithm. The traditional AIC definition has been modified based on a correction of the likelihood term, which includes signal dependent noise on the neural commands, and a Discrete Wavelet decomposition method for the proper estimation of the number of degrees of freedom of the model, reduced on a synergy-by-synergy and event-by-event basis. We tested the performance of our method in comparison with the most widespread ones, proving that our criterion is able to yield good and stable performance in selecting the correct model order in simulated EMG data. We further evaluated the performance of our AIC-based technique on two distinct experimental datasets confirming the results obtained with the synthetic signals, with performances that are stable and independent from the nature of the analysed task, from the signal quality and from the subjective EMG pre-processing steps.**

***Index Terms*— Muscle Synergies, Non-negative Matrix Factorization, Akaike Information Criterion**

I. Introduction

MUSCLE synergy analysis (MSA) is a powerful framework for characterizing the human motor control strategies. MSA works by hypothesizing that the central nervous system controls in a modular fashion all the muscles involved in a particular motor task [1]-[3].

This article was submitted on April 30th, 2021. Corresponding author: Simone Ranaldi.

S. Ranaldi, C. De Marchis and S. Conforto are with the Department of Industrial, Electronics and Mechanical Engineering, University Roma Tre, Rome, Italy (simone.ranaldi@uniroma3.it, cristiano.demarchis@uniroma3.it, silvia.conforto@uniroma3.it).

G. Severini is with the School of Electrical and Electronic Engineering, University College Dublin, Dublin, Ireland (giacomo.severini@ucd.ie).

Even if in literature several models have been proposed to describe such modularity [4]-[5], the synchronous synergy model is the most used and popular one [6]-[9].
In this representation, each motor module (*muscle synergy*) is described by a spatial component (*synergy vector*, W), containing the weighted contribution of each muscle to each synergy, and a set of time- varying activation coefficient (C), describing the coordinated recruitment of each group of muscles encoded in W.

Some papers have shown that the level of motor impairment in pathological conditions [10]-[12] and the evolution of functional recovery [13]-[16] are related to the number of synergies describing the motor control structure. Thus, the objective and accurate assessment of such a number is mandatory to guarantee the repeatability of the results and the applicability of the approach to a clinical environment.

From a methodological standpoint, muscle synergies can be extracted by applying a Non-Negative Matrix Factorization algorithm (NNMF) on the matrix containing the multi-muscle envelopes of the surface electromyography (sEMG) signal. The most used implementation of NNMF is the original gaussian one [17]-[18] that factorizes the matrix M (containing N_M envelopes constituted by N_S time points) by using the matrices W (N_M x k – encoded group muscles) and C (k x N_S – time varying activation coefficients) and a realization of a white and gaussian noise:

$$M = \hat{M} + \varepsilon = WC + \varepsilon \quad (1)$$

The parameter k, which is the number of muscle synergies, is generally determined on the basis of some quality parameters such as the Variance Accounted For (VAF) or coefficients of determination R^2: a number of synergies going from 1 to the number of recorded muscles are extracted, and the minimum number of synergies able to exceed some kind of threshold in the quality measure is taken as the correct rank of the low-dimensional approximation. Also, some statistical thresholding based on the low-rank approximation obtained from surrogate data have been published [9].

Recently the Akaike Information Criterion (AIC) has been proposed as an objective, information-based method for the accurate selection of the number of synergies [18]-[20]; although this method is theoretically independent from any pre-processing choice and it is very promising in standardizing MSA, neither a complete quantitative assessment nor an analysis to compare the performance with other approaches

have been presented in literature. In addition, for the classical Gaussian implementation of NNMF for MSA, the standard AIC method has been proved to yield wrong number of synergies in most cases [18][21], often leading to a systematic underestimation of the correct rank of the model; considering that the original version of NNMF is still the most used for MSA, an objective criterion for the model selection that could reinforce NNMF is of critical importance.

In this work, we want to overcome the main drawback of the AIC method applied to NNMF for MSA. Aiming at this some important methodological modifications have been applied to the traditional AIC criterion, mainly consisting of a modification of the log-likelihood function used for gaussian NNMF and of a wavelet-based approach for the evaluation of the correct number of free parameters.

The innovation applied to the criterion guarantees an accurate and objective model selection whose goodness has been tested by comparing the performance among several criteria, with both simulated and experimental data.

II. Methods

A graphical representation of the proposed algorithm is given in Fig. 1. The envelope matrix is used for estimating the signal dependent noise power, and the two matrices W and C are used for the evaluation of the log-likelihood value. At the same time, the number of elements in W is taken as the number of degrees of freedom in the spatial component, while the C matrix is processed by the wavelet-based algorithm described in the following section for the evaluation of the degrees of freedom in the time component.

A. Definition of the Akaike Information Criterion

The classical definition of the AIC is given by

$$AIC = -2\log \mathrm{L}(\hat{M}) + 2N \qquad (2)$$

where N is the total number of free parameters in the model and $\mathrm{L}(\hat{M})$ is the likelihood value for the estimation. AIC for muscle synergy extraction via classical gaussian NNMF is typically written as a function of the number of synergies *k* [18]-[19]:

$$AIC(k) = \sum_{i=1}^{N_M}\sum_{j=1}^{N_S}\frac{(M_{i,j} - \hat{M}_{i,j})^2}{\sigma_M^2} + 2k(N_M + N_S) \qquad (3)$$

where the first term is the negative log-likelihood value and the second term is proportional to the sum of the parameters in W (kN_M) and in C (kN_S). This formula is valid ~~only~~ if data are corrupted only by white gaussian noise and all the samples of W and C are independent one from the other.

In the case of motor commands, it has been shown that the control signals are corrupted by signal dependent noise. This kind of noise can be modelled as having a constant coefficient of variation (constant-CV noise) [22], so we modified the first log-likelihood term in the AIC into the following:

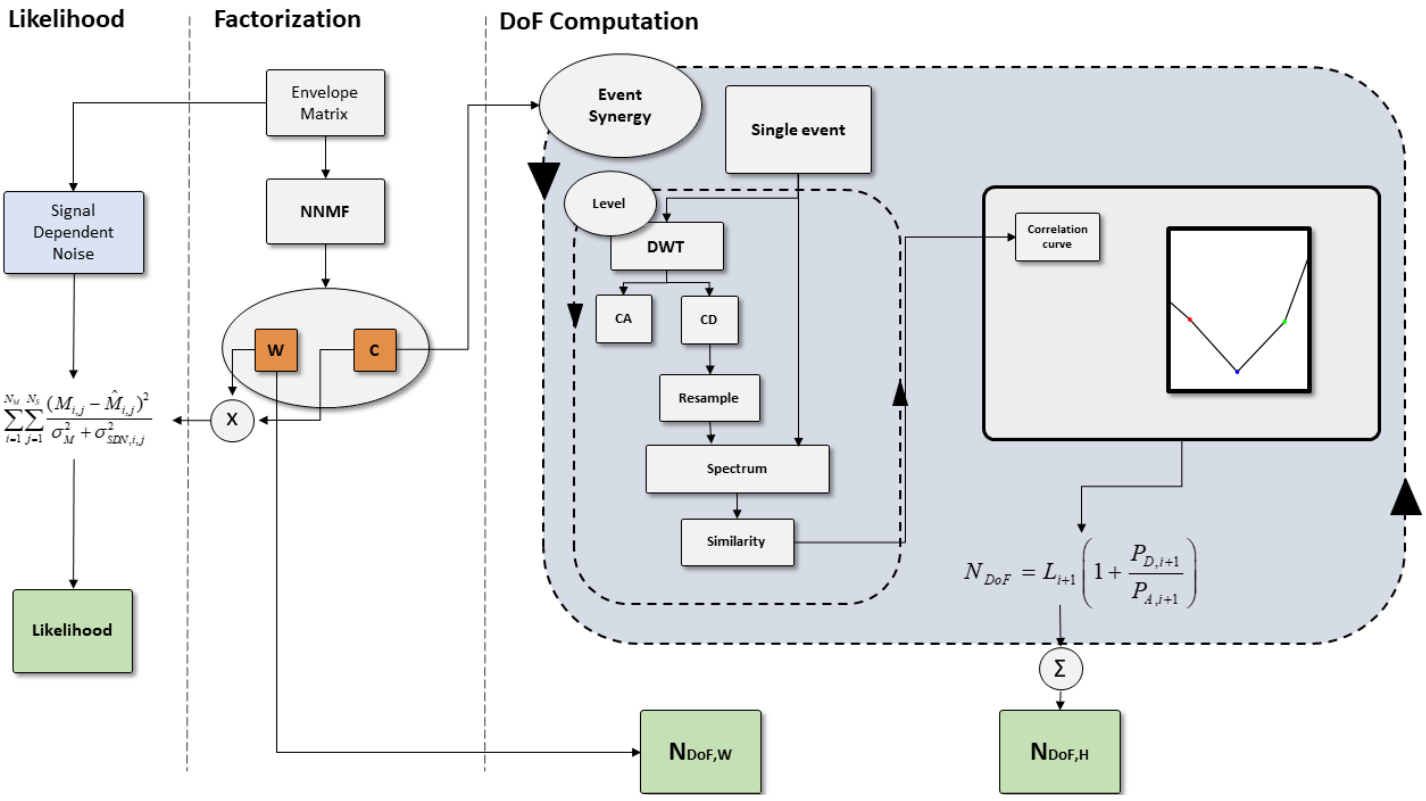

Fig 1: A graphical representation of the procedures adopted for the evaluation of the AIC

$$\log \mathrm{L}(\hat{M}) = -\frac{1}{2}\sum_{i=1}^{N_M}\sum_{j=1}^{N_S}\frac{(M_{i,j}-\hat{M}_{i,j})^2}{\sigma_M^2+\sigma^2_{SDN;i,j}} \quad (4)$$

where the term $\sigma^2_{SDN;i,j}$ takes into account an estimation of the power of the signal dependent noise on the i-th muscle at the j-th time instant. The full derivation of this quantity is given in Section II.B.

Moreover, when dealing with muscle synergy analysis, the matrix M is composed of sEMG envelopes; these signals, which are obtained from the raw sEMG, maintain the same sampling frequency of the original signal, that is over dimensioned considering the envelope frequency content. This implies that the samples of each envelope are not all independent and that in AIC the number of degrees of freedom in time is lower than $2kN_S$.

To evaluate the correct number of free parameters we considered a set of power spectra of the activation signals as obtained after a wavelet decomposition applied on each row of the activation coefficients matrix C. The full description of this method is given in Section II.C.

The modified version of the AIC has then been expressed as follows:

$$AIC(k) = -\log \mathrm{L}(\hat{M}) + 2kN_M + 2\sum_{i=1}^{k}\sum_{j=1}^{L_e}N_{DoF;i,j} \quad (5)$$

Where $N_{DoF;i,j}$ is the estimated number of free parameters for each event and each synergy, N_M is the number of muscles and L_e is the number of events. In this formulation an event is defined as one cycle, for cyclical task, or one movement for non-cyclical tasks; since most of the analyses on muscle synergies rely on the repetition of several movements this choice has been made in order to extract correctly only the degrees of freedom related to the frequency content of the muscle activations alone, without taking into account the periodical or quasi-periodical nature of movement repetitions.

This resulting formula for the AIC takes into account both a more realistic model of the noise present in the data (represented by the modified variance term in the log-likelihood formula) and an accurate computation of the free parameters of the model ($N_{DoF;i,j}$).

B. *Signal dependent noise*

For deriving a model of the signal dependent noise, we used the constant CV hypothesis given in [22]; since the variance of the signal dependent noise in motor commands has been shown to be

$$\sigma^2_{SDN} = (c\mu_S)^2 \quad (6)$$

where μ_S is the estimated mean of the distribution and c is a value between 0.1 and 0.25, we approximated the signal dependent noise power with

$$\sigma^2_{SDN,i,j} = \left(c\,\bar{S}_{i,j}\right)^2 \quad (7)$$

where $\bar{S}$ is a smoothed version of each sEMG envelope and c is a random value between 0.1 and 0.25. For smoothing, we used a time constant equal to $1/f_{peak}$, where f_{peak} is the median peak frequency of the amplitude envelope across all the events or cycles.

After the estimation of the sample-by-sample signal dependent noise power, we inserted this value into the likelihood function, so considering the noise for the i-th sample of the j-th muscle to be white and gaussian with a variance that is given by

$$\sigma^2_{i,j} = \sigma^2_M + \sigma^2_{SDN,i,j} \quad (8)$$

C. *Wavelet-based method for the selection of the correct number of free parameters*

The first step of muscle synergy analysis is the estimation of the point-by-point sEMG amplitude (i.e. the extraction of the envelope); the amplitude signal can be extracted from the rectified version of the signal by some fixed or adaptive time constant filters. It has been demonstrated that the maximum meaningful frequency contained in the rectified sEMG is significantly lower than the maximum frequency allowed by the typical 1 or 2 kHz sampling frequencies needed for correctly sampling the original signal [23]; considering this, every kind of optimal low pass filter for amplitude estimation has a cut-off frequency that is approximately lower than 30 Hz [24]. The commonly used sEMG envelopes (and so the synergy activation profiles) can be considered to be always oversampled, resulting in the need for a procedure for selecting the correct number of degrees of freedom for AIC (i.e. the minimum number of samples able to describe correctly the activation coefficients of each synergy).

For the application in the computation of the AIC, we derived a rough estimation of the correct number of degrees of freedom using a procedure based on a discrete wavelet decomposition of the signal using a Daubechies 5 wavelet. At each decomposition level *h*, we resampled the detail coefficients so as to have the same number of samples for both the original signal and the wavelet coefficients.

We then calculated a function whose values are obtained from the correlation coefficient of all (from 0 to $f_s/2^n$; f_s: sampling frequency) the portions of the normalized spectra of the detail coefficients and the one of the original signal. Since the detail coefficients at the level *h+1* are a high pass filtered version of the approximation at level *h* that has been shifted to baseband, this means to compare the frequency content at the level *h* with its high pass filtered version across all the level *h* bandwidth. In the case of sEMG signal, this function has been found to have a minimum in correspondence with the approximation level at which some of the power of the signal is transferred into the detail coefficients. A semi-quantitative proof of the presence of this minimum is given in Appendix C.

This article has been accepted for publication in a future issue of this journal, but has not been fully edited. Content may change prior to final publication. Citation information: DOI 10.1109/TNSRE.2021.3134763, IEEE Transactions on Neural Systems and Rehabilitation Engineering

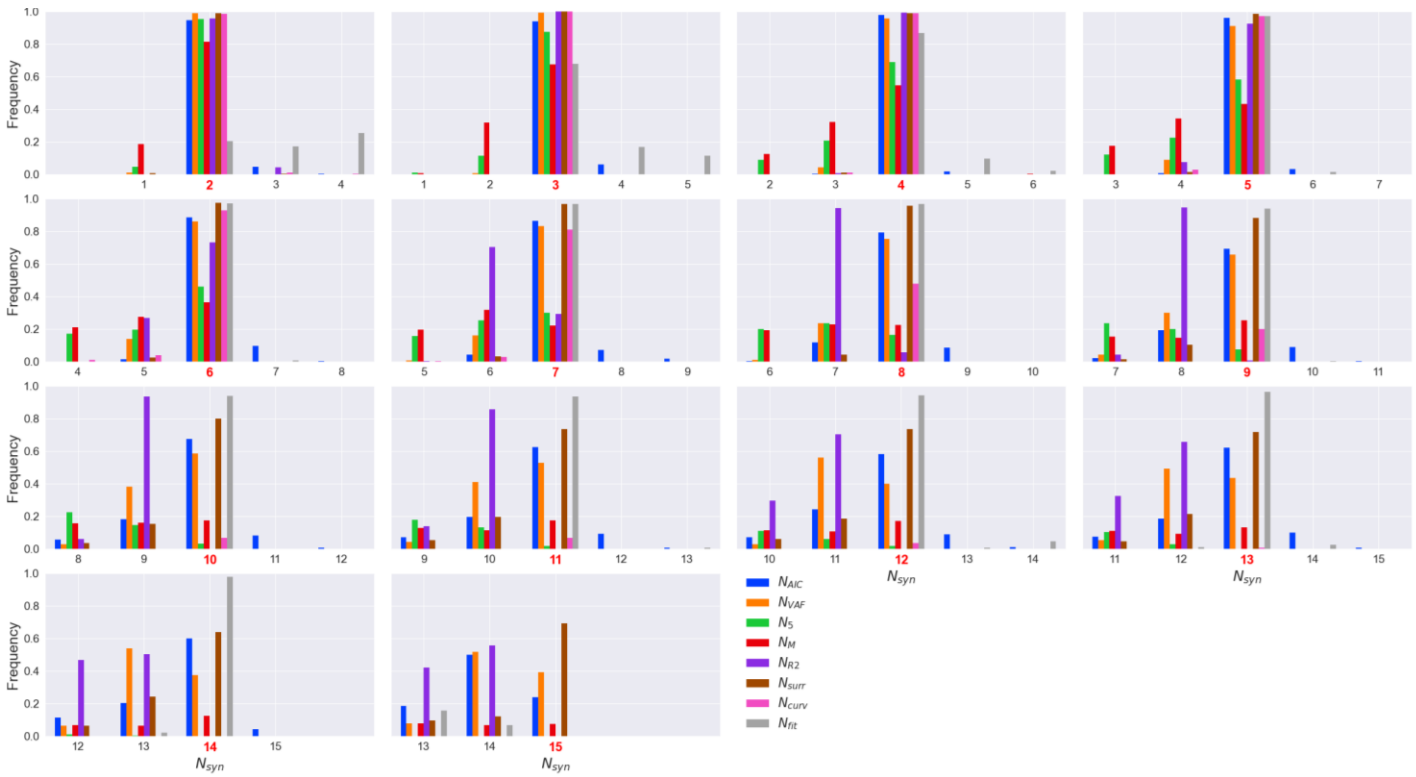

Fig. 2. Distribution of the identified number of synergies for the analysis on simulated data. Results are calculated across all the pre-processing (i.e. cut-off frequency and SNR range) conditions and shown only around the true number of synergies (indicated in red).

The advantage of using a wavelet-based method arises from the fact that it works with quadrature mirror filters (i.e. the effect of the filter on each approximation and detail signal is approximately the same) and that it implements automatically a down-sampling of the signal, so that the approximation is automatically an optimal representation of the signal. Considering this, if the minimum of the aforementioned curve is at the h-th level, we defined the correct number of free samples to be:

$$N_{DoF;i,j} = L_{h+1}\left(1+\frac{P_{D,h+1}}{P_{A,h+1}}\right) \quad (9)$$

where L_i represents the length of the detail coefficients at the h-th level. This relationship takes into account the total power P_A and P_D of the approximation and detail coefficients at each decomposition level and defines the number of degrees of freedom considering the nature of the signal included in each frequency band.

The total number of free parameters for the model is then defined as the sum across all the muscles and all the events or cycles of the so defined degrees of freedom.

D. Comparison with other model selection criteria

For a comparison between our method N_{AIC} and the solutions already proposed in literature we used several different approaches, widely used in previous research:

- Hard threshold on VAF value (**N_{VAF}**) [25]
- Hard threshold on R^2 value (**N_{R2}**) [13]
- Hard threshold on single-muscle VAF value (**N_M**) [10]
- If the increase in VAF value from n to n+1 synergies is lower than 5%, n is selected as the correct number of modules (**N_5**). This method is a global implementation of what has been proposed in [10]
- Comparison with surrogate data: if the increase in VAF going from n to n+1 synergies is lower than the 75% of the one found with the same number of modules in the decomposition of a matrix composed of random data with the same amplitude distribution, n is selected as the correct number of synergies (**N_{SURR}**) [9]
- Threshold on the curvature of any three consecutive points of the VAF curve (**N_{CURV}**) [29]
- Threshold on the goodness of the linear fit of the points of the VAF curve starting from any number of synergies (**N_{FIT}**) [30]

VAF and R2 are defined as

$$VAF = 1 - \frac{\sum\sum(M-\hat{M})^2}{\sum\sum M^2} \quad (10)$$

$$R^2 = 1 - \frac{\sum\sum(M-\hat{M})^2}{\sum\sum(M-\bar{M})^2} \quad (11)$$

The thresholds for N_{VAF} and N_{R2} have been optimized using the simulated data, varying them within the range [0.75-0.99] with steps of 0.05, and they have been set to 0.97 and 0.95

respectively; the same threshold applied to N_{VAF} has been used also for N_M. The optimization has been made in order to have high performance on average across all the simulation conditions.

Both simulated and experimental data have been used for the comparison. In particular, simulated data have been used to assess the accuracy of N_{AIC} with a controlled and varying number of muscle synergies, while the test on experimental data has been introduced to check if our criterion is able to give precise results in different tasks, experimental conditions and pre-processing steps.

E. Simulated data

In silico data have been simulated from 15 muscles which activations were generated by a known number of synergies N_{syn} ranging from 2 to 15.

The activation coefficients C have been generated with a Hann window of length uniformly chosen between 150 and 200 samples (equivalent length: 150-200 ms by hypothesizing 1kHz sampling frequency); the distance between the activations of two different synergies was set to have a minimum value of 50 samples (equivalent length: 50 ms). The Hann function is given by the relation

$$w(x) = cos^2 \frac{\pi x}{L} \qquad (12)$$

and has been chosen to simulate bell-shaped physiological activations. The corresponding C profiles have then a length that is increasing when the number of synergies is higher in order to maintain separation across the different activations.

The corresponding synergy vectors W were generated as to have a random number of active muscles between 1 and 2 N_m/N_s and a maximum correlation value of 0.6 among distinct synergy vectors. This last condition was needed to ensure that the activity of all the modules was significant in describing correctly the data, meaning that a wrong estimation of the correct number of synergies would on average lead to a bad approximation of the activity of at least one muscle.

After the definition of the envelope matrix as M = WC, we introduced signal dependent noise according to the model described in Section II.B, and each muscle activation profile was used for generating a synthetic sEMG signal following the model proposed by Stulen and De Luca [27] at a theoretical sampling frequency of 1 kHz; white gaussian noise was added on the generated signal as to have controlled SNR values. For testing the criteria in different SNR scenarios, we defined three ranges:

- 2 to 5 dB (**High-noise**)
- 7 to 10 dB (**Med-noise**)
- 15 to 18 dB (**Low-noise**)

We carried out a simulation composed of 30 realizations for each SNR range; the SNR value for each generated sEMG signal was set to a random uniform value between the two limits and was calculated as if no concurrent signal dependent noise was present; for simulated data, the equivalent power of the signal dependent noise is negligible with respect to these levels of simulated noise so that this choice is coherent with the assumptions of the algorithms. For each realization, we extracted the linear envelope to be decomposed via NNMF using rectification and low pass filtering at different frequencies (5, 10 and 20 Hz, using a 3rd order Butterworth filter).

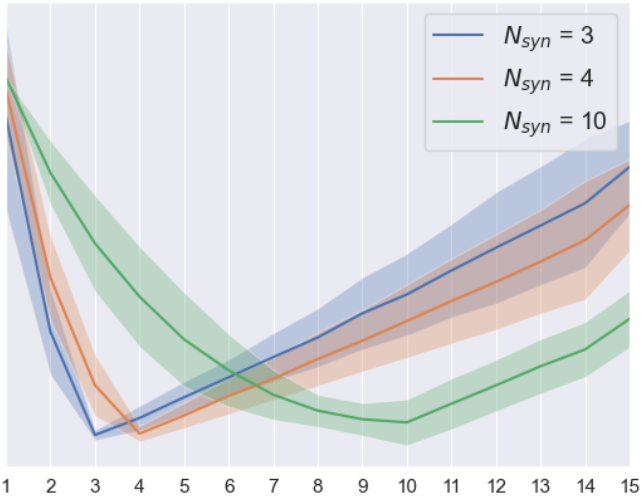

Fig. 3. Average AIC versus N_{syn} curves for 3, 4 and 10 synergies.

F. Experimental data

For the test on the experimental data, we used two different datasets consisting of the sEMG activity recorded from two different tasks. These datasets were chosen as representative of two potentially distinct motor control strategies, with different constraints and nature of the task:

- Pedalling (**ROME** dataset): this dataset is composed of the activity of 8 unilateral lower limb muscles (*Rectus Femoris*, *Vastus Medialis*, *Vastus Lateralis*, *Tibialis Anterior*, *Gluteus Maximus*, *Biceps Femoris*, *Soleus*, *Gastrocnemius Medialis*) during pedalling at a fixed cadence (60 RPM) from 9 healthy subjects. The complete description of the experimental protocol is given in [8]. This dataset was included for testing the behaviour of the AIC criterion in the case of a lower limb cyclical dynamic task with quasi-periodic muscle activations.
- Isometric upper limb (**DUBLIN** dataset): this dataset is composed of the activity of 13 unilateral upper limb muscles (*Brachiradialis, Biceps brachii short and long head, Triceps brachii lateral and long head, anterior, medialis and posterior Deltoid, Pectoralis major, Trapezius, Infraspinatus, Teres major and Latissimus dorsi*) from 14 subjects. The full description of the task and experimental protocol is given in [28]; this dataset is included as a test of the performance when dealing with upper limb isometric, non-periodic, activations.

The signals composing the ROME dataset were sampled at 1

kHz, while the DUBLIN data are sampled at 2 kHz. Envelopes were extracted using the same procedures used for the synthetic signals, and each event (for DUBLIN) or cycle (for ROME) was time-normalized to 128 and 256 samples for both datasets, to increase the speed and reliability of the wavelet method, due to the dyadic nature of the reduction of degrees of freedom at each step of the wavelet decomposition.

G. Quantification of the performance

Accuracy of the model selection criteria has been defined as the percentage of the correct identification of the number of synergies for each combination of SNR level, number of synergies and cut-off frequency (for simulated data) and of resampling length and cut-off frequency (for experimental data). The accuracy is then calculated, for each combination of parameters as the number of the correct identifications divided by the number of attempts (i.e. the number of replicates for simulated data and number of subjects for experimental signals).

The dependency of the accuracy on the processing choices has been tested with a three-way ANOVA test, with cut-off frequency, SNR level and true number of synergy as factors for simulated data and cut-off frequency, resample length and dataset (i.e. ROME and DUBLIN) for experimental signals. In order to meet the assumptions of the ANOVA test, variances of the data have been stabilized by using an arc-sine square root transformation on the values and the normality of the residuals has been checked.

III. Results

A. Simulated data

The results in Fig. 2 show the distribution of the N_{syn} identified by all the methods across all the conditions (SNR and cut-off frequency). An example of the AIC curve for different true values of the number of synergies is shown in Fig. 3.

The results in Table I and II show the accuracy as a function of the cut-off frequency for the envelope (average across the three SNR values), and the same results considered as a function of the SNR range (average across all the cut-off frequencies).

TABLE I
ACCURACY (%) FOR DIFFERENT CUT-OFF FREQUENCIES ON THE SIMULATED DATASET

	5Hz	10Hz	20Hz
N_{AIC}	71.03	78.10	73.81
N_M	28.17	32.30	33.49
N_{SURR}	72.46	91.59	94.52
N_{VAF} *	49.84	73.73	83.57
$N_{5\%}$	21.90	32.30	35.00
N_{R2}	32.14	35.32	38.89
N_{CURV}	42.06	49.37	48.73
N_{FIT}	79.76	84.05	78.89

In Table III, the descriptive statistics of the accuracies for each processing scenario and SNR level and for all the simulated N_{syn} are shown; since the performance of any algorithm are dependent ($p<0.05$) on the true number of synergies when the data are generated by a high number of modules, we tested with this measure the overall stability of the criteria as a function of the processing choices and the SNR, not the number of synergies. The AIC criterion has the most stable performance across all the conditions ($p>0.05$ for all the conditions), being either the best performing or comparable with the best performing one, having in some conditions lower accuracy with respect to N_{SURR}. Statistical dependency on the highlighted factor has been marked in Table I and II with an asterisk.

TABLE II
ACCURACY (%) FOR DIFFERENT SNR RANGES ON THE SIMULATED DATASET

	High-Noise	Med-Noise	Low-Noise
N_{AIC}	72.78	74.84	75.32
N_M	26.9	33.49	33.57
N_{SURR} *	94.52	88.17	75.87
N_{VAF} *	41.67	74.68	90.79
$N_{5\%}$ *	12.86	30.79	45.56
N_{R2}	35.63	35.87	34.84
N_{CURV}	46.98	46.59	46.59
N_{FIT}	70.95	84.21	87.54

TABLE III
AVERAGE, MINIMUM AND MAXIMUM ACCURACY (%) ON THE SIMULATED DATASET

	Average	Minimum	Maximum
N_{AIC}	74.31	66.19	79.29
N_M	31.32	21.90	35.95
N_{SURR}	86.19	61.43	100
N_{VAF}	69.05	21.19	98.81
$N_{5\%}$	29.74	6.90	51.43
N_{R2}	35.45	30.00	35.95
N_{CURV}	46.72	41.19	49.76
N_{FIT}	80.90	66.43	87.86

B. Experimental data

For testing the performance of the different methods with the two experimental datasets, we defined the estimated true number of synergies for each subject as the most frequent value obtained with the three most accurate criteria; the three selected criteria have been chosen as the ones able to yield a minimum accuracy higher than the 50% on the whole simulated dataset, namely N_{AIC}, N_{SURR} and N_{FIT}.

TABLE IV
ACCURACY (%) FOR DIFFERENT CUT-OFF FREQUENCIES (EXPERIMENTAL DATASETS)

	ROME			DUBLIN		
	5Hz	10Hz	20Hz	5Hz	10Hz	20Hz
N_{AIC}	68.75	75.00	62.5	60.71	57.14	60.71
N_M *	25.00	12.50	0	0	0	0
N_{SURR}	50.00	56.25	65.5	71.43	82.14	75.00
N_{VAF} *	75.00	25.00	0	21.43	0	0
$N_{5\%}$	50.00	50.00	50.00	14.29	14.29	28.57
N_{R2} *	62.50	75.00	37.50	35.71	7.14	0
N_{CURV} *	87.5	87.5	81.25	50.00	39.29	28.57
N_{FIT}	50.00	56.25	62.50	0	0	0

In Fig. 4 the average behaviour of the AIC curve for the ROME and DUBLIN subjects is shown. The two curves exhibit a pronounced minimum in correspondence of 4 synergies, coherently with previous literature [8][28].

Results for both the ROME and the DUBLIN datasets are shown in Tables IV and V. Median and IQR values are computed by calculating the subject-by-subject accuracy (i.e. the values coming from each subject and all the processing choices). Our criterion has been found to have the most stable performances across the two datasets and the processing conditions. VAF-based criteria, in contrast have a dependency on the dataset, being N_{SURR} the optimal choice on DUBLIN dataset, and N_{CURV} on ROME. The accuracy and error reported in Table IV and V are expressed with respect to the hypothesized true number of synergies.

Dependency of the accuracy on the cut-off frequency has been marked with an asterisk in Table IV. No dependency on the resample length has been found ($p>0.05$ for all the algorithms), while only N_{AIC} has independent accuracy with respect to the dataset.

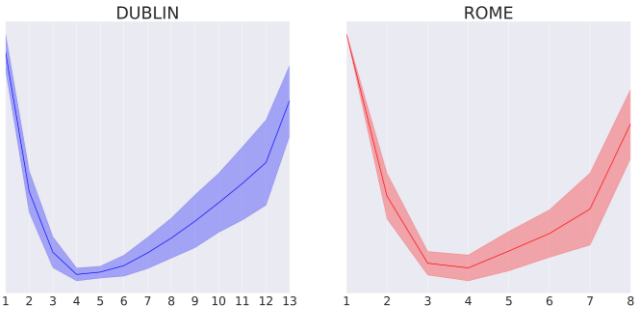

Fig. 4. Average behaviour, across all subjects and all pre-processing conditions, of the AIC versus N_{syn} curve for both the experimental datasets (ROME: dynamic, cyclical. DUBLIN: isometric, non cyclical).

TABLE V
ERROR STATISTICS (EXPERIMENTAL DATASET)

	ROME			DUBLIN		
	Median	**25th**	**75th**	**Median**	**25th**	**75th**
N_{AIC}	0	0	0	0	0	1
N_M	2	1	4	6.5	4	8
N_{SURR}	0	-1	0	0	0	0
N_{90}	1	0	2	3	2	4
$N_{5\%}$	-0.5	-1	0	-1	-1	-1
N_{R2}	0	0	1	1.5	1	3
N_{CURV}	0	0	0	-1	-2	0
N_{FIT}	0	0	1	3	3	4

IV. DISCUSSION

In this paper we proposed a method to apply the Akaike Information Criterion for the selection of the correct number of synergies to be extracted from multi-muscle sEMG recordings via the original Gaussian Non-Negative Matrix Factorization algorithm.

Previous attempts to apply this criterion to the original NNMF implementation concluded that, regardless of data structure, the minimum for the AIC was found for 1 synergy [21], and in general the application of this criterion led to an overall underestimation of the underlying number of synergies [18]-[20]; since the increasing branch of the AIC curve is given by the dominance of the degrees of freedom term over the likelihood term, such a result can derive from an overestimation of the number of free parameters, generally due to oversampling. We modified this part of the AIC criterion to take into account the characteristics of the sEMG envelope, by evaluating an optimal subsampling procedure for each synergy activation. In doing so, we corrected the overestimation of the second term in the AIC, finding results that are independent from any processing choice.

In addition, we modified the likelihood term in AIC to take into account the physiological characteristics of the signals to be decomposed; since it has been proved [22] that neural commands are corrupted by signal dependent noise, we corrected the noise power in the model to insert an additive term that takes into account a rough estimation of the power of the neural noise. Both this and the correction on the number of free parameters yielded a corrected version of the AIC criterion that is able to identify the correct number of synergies by using the most used implementation of the NNMF algorithm.

From a general point of view, we found that our method is able to yield good results on different datasets and across all the possible true numbers of motor modules.

The analysis on simulated data proved how, although for small numbers of synergies most of the criteria have comparable performances, when no hypotheses about the maximum number of synergies can be made, N_{AIC}, N_{FIT} and N_{SURR} represent the safest choices for the definition of the dimensionality of the model.

The analysis on the two experimental datasets, proved that also when dealing with real sEMG signals, N_{AIC} has independent performance from the nature of the data, while the other best performing algorithms, namely N_{SURR} and N_{CURV} fail to maintain a stable performance over the two scenarios.

Between the two datasets, ROME is the one that has in general the lowest error across all the criteria; this is mainly due to the fact that the envelopes are quasi-periodical, and all the corresponding synergies are activated with very regular shapes. DUBLIN, in contrast is more challenging, considering its non-periodical nature; the lower regularity of the task results in a worsening of the precision of most of the criteria, suggesting that for the selection of the optimal processing scheme some a priori knowledge on the activations is needed. It has to be remarked that the results on the two datasets depend on the method used for defining the true number of synergies; our strategy, however, exploits the results from the best performing algorithms to extract this information, aiming to a stable and reliable comparison. Moreover, the estimated true number of synergies is coherent with previous results that have been published on the same dataset, varying between 3 and 5.

Threshold-based criteria have here been tested with optimized values based on the simulated data; this optimization is possibly not valid also for our experimental data, hence the low accuracies reported. While a different optimization can improve the performance of N_{VAF}, N_{R2} and N_M, this dependency is alone a disadvantage of these methods over all the others. In the literature, the threshold is typically set to 90% for VAF values and in most cases requires some additional heuristic analysis to determine the correct number of synergies; for this reason, the analysis with this threshold has not been included

here.

N_{SURR}, $N_{5\%}$, N_{CURV} and N_{FIT} all attempt to find the elbow of the VAF curve; all these methods also apply a threshold on some curvature or slope measure so that the very same consideration can be applied also on those algorithms. N_{SURR}, however, apart from the subjective 0.75 threshold on the slope, exploits statistical features of the signal and has a working principle that is closer to N_{AIC} with respect to all the other selection methods in terms of independence from subjective choices. All the tested criteria can be applied on both VAF and R^2 curves, with different thresholds; in this work we selected the most used strategies to benchmark the performance of N_{AIC} in order to yield a characterization of its accuracy with respect to the current scientific literature on the topic.

Our information-based criterion is tuned on the general characteristics of the signals used in the analysis and is not dependent on any threshold; this, together with the good performance reached with all the tested data, support the proposal of our AIC criterion as a standard method for selecting the correct number of muscle synergies from any kind of multi-muscle sEMG recordings. In the literature, several alternative methods for an automatic detection of the number of synergies have been proposed [31]-[33]; all the techniques, however, exploit different assumptions on the task or the neurophysiological significance of the W and C components. In our proposed technique, in contrast, the number of a priori assumptions on the underlying model of the signal was minimized; a fine tuning of the model parameters could lead to further improvements of the method, even though a more complex definition of the likelihood term could be required. The present methodology was implemented for the synchronous muscle synergy model, but an Akaike Information Criterion could be fitted ad-hoc for other modular motor control models, such as the one based on fixed temporal components [5][26] or the time varying muscle synergies approach [3].

V. Conclusions

In this paper, we proposed a method for the evaluation of the Akaike Information Criterion for the selection of the number of muscle synergies to be extracted from multi-muscle surface EMG recordings. Our implementation is based on both the definition of a model for the log-likelihood function and on a procedure for the calculation of the number of free parameters in the synergy model. We proved that our method has good performance in the identification of the correct number of modules in both simulated and experimental conditions, independently from any pre-processing choices; considering this, our AIC can represent a good solution for the improvement of the repeatability and reliability of muscle synergy analyses results.

Appendix

A. Proof of the behaviour of the correlation curve

An approximation of the sEMG envelope spectrum can be built as:

$$P(f) = \begin{cases} 0 & f < f_1 \\ 1 & f_1 < f < f_2 \\ 0 & f > f_2 \end{cases} \quad (13)$$

With this approximation the correlation coefficient can be written as proportional to

$$N_{overlap} - \frac{1}{F_m} N_{up,s} N_{up,d} \quad (14)$$

With $F_M = \frac{f_s}{2^n}$, $N_{overlap}$ the number of overlapped high samples and $N_{up,s}$ and $N_{up,d}$ the number of samples equal to 1 in the signal portion and detail coefficient spectra, respectively.

This quantity is decreasing with the decomposition levels before the maximum frequency of the signal considering the fact that $N_{overlap}$ is 0 and $\frac{1}{F_m} N_{up,s}$ is higher the lower F_M. When F_M is lower than f_1, the quantity is increasing with the approximation levels, being $N_{overlap}$ and $N_{up,s}$ equal to 0 and $N_{up,d}$ decreasing.

If at a certain decomposition level $N_{overlap}$ is higher than 0, the value of the correlation is increasing with respect to the previous level.

Considering these three trends of the curve, the correlation is expected to have a minimum in correspondence of the maximum frequency of the spectrum if $f_2 < f_s$.

References

[1] F. Hug, N. A. Turpin, A. Guével, and S. Dorel, "Is interindividual variability of EMG patterns in trained cyclists related to different muscle synergies?," *Journal of Applied Physiology*, vol. 108, no. 6, pp. 1727–1736, 2010

[2] Neptune, R. R., Clark, D. J., & Kautz, S. A. (2009). Modular control of human walking: a simulation study. Journal of biomechanics, 42(9), 1282-1287.

[3] d'Avella, A., Portone, A., Fernandez, L., & Lacquaniti, F. (2006). Control of fast-reaching movements by muscle synergy combinations. Journal of Neuroscience, 26(30), 7791-7810.

[4] I. Delis, P. M. Hilt, T. Pozzo, S. Panzeri, B. Berret, B. "Deciphering the functional role of spatial and temporal muscle synergies in whole-body movements". *Scientific reports*, 8(1), 1-17. 2018

[5] D. Torricelli, C. De Marchis, A d'Avella, D.N. Tobaruela, F. O. Barroso, J. L Pons. "Reorganization of muscle coordination underlying motor learning in cycling tasks". *Frontiers in Bioengineering and Biotechnology*, 8.2020

[6] Augenstein, T. E., Washabaugh, E. P., Remy, C. D., & Krishnan, C. (2020). Motor Modules are Impacted by the Number of Reaching Directions Included in the Analysis. IEEE Transactions on Neural Systems and Rehabilitation Engineering, 28(9), 2025-2034.

[7] M. Ghislieri, V. Agostini, M. Knaflitz. "Muscle synergies extracted using principal activations: improvement of robustness and interpretability". *IEEE Transactions on Neural Systems and Rehabilitation Engineering*, 28(2), 453-460, 2020.

[8] C. De Marchis, M. Schmid, D. Bibbo, I. Bernabucci, and S. Conforto, "Inter-individual variability of forces and modular muscle coordination in cycling: A study on untrained subjects," *Human Movement Science*, vol. 32, no. 6, pp. 1480–1494, 2013.

[9] V. C. K. Cheung, L. Piron, M. Agostini, S. Silvoni, A. Turolla, and E. Bizzi. "Stability of muscle synergies for voluntary actions after cortical stroke in humans." *Proceedings of the National Academy of Sciences*: pnas-0910114106. 2009

[10] D. Clark, L. Ting, F. Zajac, R. Neptune and S. Kautz, "Merging of Healthy Motor Modules Predicts Reduced Locomotor Performance and Muscle Coordination Complexity Post-Stroke", *Journal of Neurophysiology*, vol. 103, no. 2, pp. 844-857, 2010.

[11] E. Ambrosini, C. D. Marchis, A. Pedrocchi, G. Ferrigno, M. Monticone, M. Schmid, T. D'Alessio, S. Conforto, and S. Ferrante, "Neuro-Mechanics of Recumbent Leg Cycling in Post-Acute Stroke Patients," *Annals of Biomedical Engineering*, vol. 44, no. 11, pp. 3238–3251, Jan. 2016.

[12] K. Kubota, H. Hanawa, M. Sonoo, S. Kita, K. Hirata, T. Fujino, T. Kokubun, T. Ishibashi, N. Kanemura. "Usefulness of Muscle Synergy Analysis in Individuals with Knee Osteoarthritis during Gait". *IEEE Transactions on Neural Systems and Rehabilitation Engineering*.

[13] V. C. K.Cheung, A. Turolla, M. Agostini, S. Silvoni, C. Bennis, P. Kasi, S. Paganoni, P. Bonato, and E. Bizzi. "Muscle synergy patterns as physiological markers of motor cortical damage." *Proceedings of the National Academy of Sciences* 109, no. 36: 14652-14656. 2012

[14] R. L. Routson, D. J. Clark, M. G. Bowden, S. A. Kautz, R. R. Neptune, "The influence of locomotor rehabilitation on module quality and post-stroke hemiparetic walking performance". *Gait & posture*, vol. 38, no. 3, pp. 511-517, 2013.

[15] C. De Marchis, S. Ranaldi, M. Serrao, A. Ranavolo, F. Draicchio, F. Lacquaniti, S. Conforto. "Modular motor control of the sound limb in gait of people with trans-femoral amputation". *Journal of neuroengineering and rehabilitation*, vol. 16, no. 1, pp. 1-11. 2019

[16] E. Ambrosini, M. Parati, E. Peri, C. De Marchis, C. Nava, A. Pedrocchi, G. Ferriero, S. Ferrante. "Changes in leg cycling muscle synergies after training augmented by functional electrical stimulation in subacute stroke survivors: a pilot study". *Journal of neuroengineering and rehabilitation*, 17(1), 1-14.

[17] D. D. Lee and H. S. Seung, "Learning the parts of objects by non-negative matrix factorization," *Nature*, vol. 401, no. 6755, pp. 788–791, 1999.

[18] K. Devarajan and V. Cheung, "On Nonnegative Matrix Factorization Algorithms for Signal-Dependent Noise with Application to Electromyography Data", *Neural Computation*, vol. 26, no. 6, pp. 1128-1168, 2014.

[19] V. C. K. Cheung, K. Devarajan, G. Severini, A. Turolla, and P. Bonato, "Decomposing time series data by a non-negative matrix factorization algorithm with temporally constrained coefficients," *2015 37th Annual International Conference of the IEEE Engineering in Medicine and Biology Society (EMBC)*, 2015.

[20] G. Severini, & C. De Marchis. "Effect of SNR normalization on the estimation of muscle synergies from EMG datasets" In *2018 IEEE International Symposium on Medical Measurements and Applications (MeMeA)* (pp. 1-5). IEEE, 2018.

[21] A. Santuz, A. Ekizos, L. Janshen, V. Baltzopoulos, and A. Arampatzis, "On the Methodological Implications of Extracting Muscle Synergies from Human Locomotion," *International Journal of Neural Systems*, vol. 27, no. 05, p. 1750007, 2017.

[22] C. M. Harris and D. M. Wolpert, "Signal-dependent noise determines motor planning," *Nature*, vol. 394, no. 6695, pp. 780–784, 1998.

[23] L. Myers, M. Lowery, M. Omalley, C. Vaughan, C. Heneghan, A. S. C. Gibson, Y. Harley, and R. Sreenivasan, "Rectification and non-linear pre-processing of EMG signals for cortico-muscular analysis," *Journal of Neuroscience Methods*, vol. 124, no. 2, pp. 157–165, 2003.

[24] S. Ranaldi, C. D. Marchis, and S. Conforto, "An automatic, adaptive, information-based algorithm for the extraction of the sEMG envelope," *Journal of Electromyography and Kinesiology*, vol. 42, pp. 1–9, 2018.

[25] Tresch, M.C., Saltiel, P., and Bizzi, E.. "The construction of movement by the spinal cord." *Nature neuroscience* 2.2, pp.162-167, 1999.

[26] Y. P. Ivanenko, R. E. Poppele, and F. Lacquaniti, "Five basic muscle activation patterns account for muscle activity during human locomotion," *The Journal of Physiology*, vol. 556, no. 1, pp. 267–282, 2004.

[27] F. B. Stulen and C. J. D. Luca, "Frequency Parameters of the Myoelectric Signal as a Measure of Muscle Conduction Velocity," *IEEE Transactions on Biomedical Engineering*, vol. BME-28, no. 7, pp. 515–523, 1981.

[28] De Marchis, C., Di Somma, J., Zych, M., Conforto, S. and Severini, G., 2018. "Consistent visuomotor adaptations and generalizations can be achieved through different rotations of robust motor modules". *Scientific Reports*, 8(1).

[29] Cheung, V., 2005. Central and Sensory Contributions to the Activation and Organization of Muscle Synergies during Natural Motor Behaviors. *Journal of Neuroscience*, 25(27), pp.6419-6434.

[30] Tresch, M., Cheung, V. and d'Avella, A.. "Matrix Factorization Algorithms for the Identification of Muscle Synergies: Evaluation on Simulated and Experimental Data Sets". *Journal of Neurophysiology*, 95(4), pp.2199-2212, 2006.

[31] Delis, I., Berret, B., Pozzo, T. and Panzeri, S.. "A methodology for assessing the effect of correlations among muscle synergy activations on task-discriminating information". *Frontiers in Computational Neuroscience*, 7, 2013.

[32] Kim, Y., Bulea, T. and Damiano, D.. "Novel Methods to Enhance Precision and Reliability in Muscle Synergy Identification during Walking". *Frontiers in Human Neuroscience*, 10, 2016.

[33] Ballarini, R., Ghislieri, M., Knaflitz, M., and Agostini, V.. "An Algorithm for Choosing the Optimal Number of Muscle Synergies during Walking". *Sensors*, 21(10), 3311, 2021.